Effect of Styrene–Isoprene–Styrene, Styrene–Butadiene–Styrene, and Styrene–Butadiene–Rubber on the Mechanical, Thermal, Rheological, and Morphological Properties of Polypropylene/Polystyrene Blends

P. Raghu, C. K. Nere, R. N. Jagtap

Department of Chemical Technology, University of Mumbai, PPV Division, Matunga, Mumbai 400 019, India

Received 10 December 2001; accepted 24 April 2002

ABSTRACT: The mechanical, thermal, rheological, and morphological properties of polypropylene (PP)/polystyrene (PS) blends compatibilized with styrene–isoprene–styrene (SIS), styrene–butadiene–styrene (SBS), and styrene–butadiene–rubber (SBR) were studied. The incompatible PP and PS phases were effectively dispersed by the addition of SIS, SBS, and SBR as compatibilizers. The PP/PS blends were mechanically evaluated in terms of the impact strength, ductility, and tensile yield stress to determine the influence of the compatibilizers on the performance properties of these materials. SIS- and SBS-compatibilized blends showed significantly improved impact strength and ductility in comparison with SBR-compatibilized blends over the entire range of compatibilizer concentrations. Differential scanning calorimetry indicated compatibility between the components upon the addition of SIS, SBS, and SBR by the appearance of shifts in the melt peak of PP toward the melting range of PS. The melt viscosity and storage modulus of the blends depended on the composition, type, and amount of compatibilizer. Scanning electron microscopy images confirmed the compatibility between the PP and PS components in the presence of SIS, SBS, and SBR by showing finer phase domains. J Appl Polym Sci 88: 266–277, 2003

Key words: poly(propylene) (PP); polystyrene; blends; compatibility; mechanical properties; rheology; morphology

INTRODUCTION

Polymer blends have gained considerable importance in recent years because of the possibility of improvements in the properties by the suitable selection of ingredients and their ratios. Nowadays, polymer blends are considered among the most important developments in polymer engineering because of a number of successful applications. The blending of polymers offers a facile method to produce new materials with tailor-made properties and versatility that vary with the miscibility or other properties of the constituents. Polypropylene (PP) and polystyrene (PS) have been known for years as commodity plastics with many desired properties. PP possesses a good balance of properties, such as excellent chemical resistance, good oxygen barrier properties, good environmental stress crack resistance, and easy processability, and its moderate cost and light weight also contribute to its value and versatility. However, PP has some drawbacks associated with its poor thermoformability, high mold shrinkage, and dimensional instability due to its inherent properties of rapid crystallization and poor printability. PS has some advantages over PP in its low mold shrinkage, excellent printability, and broad thermoforming processing window, even if its other mechanical and thermal properties are not as good as those of PP. The blending of PP and PS may, therefore, offset the drawback of each polymer, leading to a new approach for PP in various commercial applications.

Most polymer blends are not compatible without the addition of a third component known as a compatibilizer,[1–5] and PP/PS blends are no exception. The simple blending of incompatible polymer such as PP and PS generally results in poor properties because of their unfavorable molecular interactions. To overcome this problem, researchers have studied the introduction of compatibilizers for decades. The use of styrene/ethylene-*co*-butadiene/styrene (SEBS), styrene–butadiene–styrene (SBS), styrene–isoprene–styrene (SIS), and propylene-*g*-styrene copolymer has effectively improved the mechanical properties and dispersion over those of noncompatibilized PP/PS blends.[6–15] Iwala et al.[16] studied the morphology and mechanical properties of PP/PS blends with PP as the major phase and with SEBS as a compatibilizer. The morphology of the resulting blend was similar to that of an interpenetrating polymer network and showed an improved dispersion of one polymer into the other and improved interfacial adhesion between the two polymers. Pluta et al.[17] studied the morphology and

Correspondence to: R. N. Jagtap (jagtap@ppv.udct.ernet.in).
Contract grant sponsor: University Grants Commission.

dynamic mechanical properties of PP/PS blends of similar compositions but of various degrees of dispersion. The blends containing *in situ* polymerized PS showed the presence of nanoscale phase separation of PS, whereas the blends prepared by melt mixing showed the physical entanglement of the PS phase and noncrystalline PP phase in the macrosize domain. Both blend systems showed the dependence of the viscoelastic behavior on the dispersions of PS inclusions and on the nature of the interface. Rablej et al.[18] studied the crystallinity of PP/PS blends over a wide composition range. Their results indicated that when PP was the major component in the blend, its crystallization behavior was not affected by its blending with PS. However, if PP was the minor component, it was dispersed well in the immiscible PS matrix, and so the nucleation mechanism changed from being predominantly heterogeneous to being a homogeneous system as long as the size of the dispersed PP droplet was below a critical value (1–2 μm). Fortelny et al.[19] studied the effect of mixing conditions on the phase structure of PP/PS blends. The size of the dispersed particle was higher for the compression-molded sample than for the quenched sample. This was caused by the coalescence and/or transfer of dispersed particles during the slower crystallization of the PP matrix. Giudice et al.[20] reported that PP/PS blends compatibilized with a PP/PS diblock with a high number-average molecular weight had properties approaching those of high-impact polystyrene (HIPS). Appleby et al.[21] studied the effectiveness of a series of block copolymer compatibilizers in improving the impact strength of PP/PS blends. The addition of only 5 wt % of a commercial PS-PB-PS triblock copolymer afforded about a threefold improvement in the impact strength for a 1:1 PP/PS blend over the noncompatibilized blend and led to an impact strength near that of HIPS. This compatibilizer was effective as a high molecular weight tapered diblock and appeared to be substantially more effective than either low molecular weight diblocks or a high molecular weight triblock. D'orazio et al.[22] studied the influence of crystallization conditions on the morphology and thermal behavior of PP/PS blends compatibilized by a novel graft copolymer of unsaturated propylene with styrene (uPP-*g*-PS). The presence of the copolymer affected the interfacial tension between the PP and PS phases in the melt state, with the PS particle size and the particle size distribution being strongly modified. Near the crystallization temperature of the PP phase, the addition of the uPP-*g*-PS copolymer induced a drastic change both in the PS mode and the state of dispersion and in the PP spherulitic texture and inner structure of the spherulite fibrils.

In this work, PP/PS blends with SIS, SBS, and styrene–butadiene–rubber (SBR) compatibilizers were prepared. The compatibilizer effect was studied by the measurement of the various material properties (mechanical, thermal, and rheological) and the morphology. The optimal blend composition associated with the desired properties may be obtained from this study.

EXPERIMENTAL

Materials

The PP used in this study was obtained from Reliance Industries, Ltd. (Mumbai, India). It was an 11 g/10 min melt-flow index (MFI) material (at 230°C/2.16 kg) known as Repol H100EY. PS was contributed by Supreme Petrochem, Ltd. (Mumbai, India), as Suprene SC 205. It was a 7.6 g/10 min MFI material (at 230°C/2.16 kg). SIS was obtained from Shell Chemicals (The Netherlands) as Kraton D-1107 CP, a material with a 10 g/10 min MFI (at 200°C/5 kg) and with bound styrene of a 15% mass. SBS was obtained from Shell Chemicals as Kraton D-1101 CS, a material with a 0.8 g/10 min MFI (at 200°C/5 kg) and with bound styrene of a 31% mass. The SBR used was Solprene 1000 obtained from Belgium Rubber Co. (Belgium) with bound styrene of an 18% mass.

Blend preparation

The blends were prepared through the melt blending of required quantities of PP, PS, and SIS, SBS, or SBR with an APV Baker twin-screw extruder (length/diameter ratio 24:1; model MP 19PC) (England) in a high-dispersive-mixing screw configuration. The granules of PP, PS, and SIS, SBS, or /SBR were hand-mixed (dry blending) in appropriate ratios before being added to the extruder. The temperatures of the five zones, from the feed zone to the die zone, of the extruder were successively 170, 180, 195, 210, and 220°C.

The screw speed was set at 80 rpm, and the melt pressures measured at the entrance to the die were 5–8 bar, depending on the material extruded. The blend extrudate was immediately quenched in water, dried, and then chopped into small pellets. The compatibilizers SIS, SBS, and SBR were incorporated into 70/30 PP/PS blends at levels of 2, 3, 5, and 10 phr. The various blend compositions prepared are shown in Table I.

Specimen preparation

The granules of the blend extrudates were predried in an air-circulating oven at 80 ± 5°C for 4 h for the elimination of moisture. Dried pellets were injection-molded with an injection-molding machine (screw diameter = 35 mm, metering stroke = 160 mm; model SP 200/80, Boolani) so that we could obtain tensile, flexural, and Izod impact test specimens. The injection

TABLE I
Blend Composition of PP/PS Systems with and Without Compatibilizer

Blend code	Blend composition		
	PP (phr)	PS (phr)	SIS/SBS/SBR (phr)
PPS73	70	30	0
SIS732	70	30	2
SIS733	70	30	3
SIS735	70	30	5
SIS7310	70	30	10
SBS732	70	30	2
SBS733	70	30	3
SBS735	70	30	5
SBS7310	70	30	10
SBS732	70	30	2
SBS733	70	30	3
SBR735	70	30	5
SBR7310	70	30	10

temperature and pressure were 230°C and 72 bar, respectively, and the cooling time was 45 s.

Testing of the mechanical properties

The tensile yield properties was measured at ambient conditions on a Lloyd LR 50 K universal testing machine (Hampshire, England) with dumbbell shaped specimens at a crosshead speed of 50 mm/min according to ASTM D 638M. The flexural properties were tested at ambient conditions on the same machine at a crosshead speed of 2.7 mm/min according to ASTM D 790M. The notched Izod impact strength was determined at ambient conditions on an Avery Denison pendulum impact tester (Leeds, England) with an impact rate of 3.46 m/s as per ASTM D 256. The linear shrinkage was determined with a Mitutoyo vernier slide caliper (Japan) according to ASTM D 955. The average values of at least five tests are reported.

Thermal property analysis

The thermal characteristics of the compatibilized PP/PS blends were studied with a PerkinElmer model 7 differential scanning calorimeter (USA). Polymer samples of 7–9 mg were sealed in an aluminum pan and heated and cooled at a rate of 10°C/min. Initially, the polymer samples were heated from room temperature to 220°C at a heating rate of 10°C/min and annealed for 1 min for the elimination of any thermal and mechanical history in the sample. They were then cooled to obtain the crystallization peaks and heated again to obtain the melting peaks.

Measurement of the activation energy of viscous flow (*E*)

The MFI of each blend composition was determined with a Davenport microprocessor-based instrument (Hampshire, England) according to ASTM D1238. The MFI was determined with a load of 2.16 kg at 180, 190, 210, and 230°C for PP/PS blends. The logarithm values of the MFI at different temperatures are plotted against the reciprocal of the temperature ($1/T$) for the calculation of E. The slope of the semilogarithmic plot of log MFI versus $1/T$ gives E at a constant shear rate.

Rheological measurements

The flow behavior of the PP/PS blends was studied by the measurement of the viscosity as a function of the shear rate with a Haake RT10 rheometer (Germany) equipped with parallel-plate geometry. The test was performed on a sample at 200°C over a shear rate range of 0.001–10 s^{-1}. The viscoelastic shear properties of PP/PS blends were also studied by the measurement of the storage modulus (G') and phase angle (tan δ) within the linear viscoelastic region of the polymers

TABLE II
Mechanical Properties and *E* Values of PP/PS Blend Compositions with and Without Compatibilizer

Blend code	Tensile properties			Flexural properties		Impact strength (J/m)	Linear shrinkage (%)	*E* (kJ/mol)
	Tensile strength (MPa)	Tensile modulus (Mpa)	Extension at break (%)	Flexural strength (MPa)	Flexural modulus (MPa)			
PPS73	36.14	1153.49	9.6	43.56	1821.42	21.78	0.951	49.93
SIS732	33.10	1104.18	108	34.26	1389.24	26.614	1.034	54.91
SIS733	31.49	988.89	140	34.62	1371.59	31.181	1.106	58.12
SIS735	30.24	934.89	154	30.33	1323.78	37.953	1.114	57.60
SIS7310	27.81	740.933	183	23.94	792.00	51.570	1.305	50.65
SBS732	35.01	1131.44	104	34.78	1475.64	24.882	1.099	63.39
SBS733	34.34	990.19	96	34.92	1457.76	27.165	1.122	62.04
SBS735	33.93	940.68	76	34.60	1413.02	30.945	1.118	67.61
SBS7310	31.43	861.93	29	27.86	1059.00	47.630	1.282	74.75
SBR732	33.08	1055.37	17.2	29.08	1204.4	22.84	1.083	46.84
SBR733	32.99	1075.86	12.6	35.34	1330.0	23.62	1.122	52.26
SBR735	30.92	1004.99	10.7	33.32	1244.0	24.81	1.145	50.57
SBR7310	28.61	944.63	9.1	28.63	1117.0	25.59	1.145	51.56

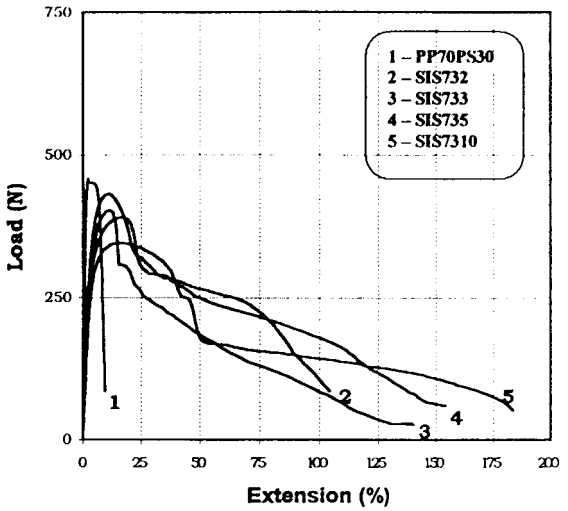

Figure 1 Load–extension curves of the SIS-compatibilized 70/30 PP/PS blends.

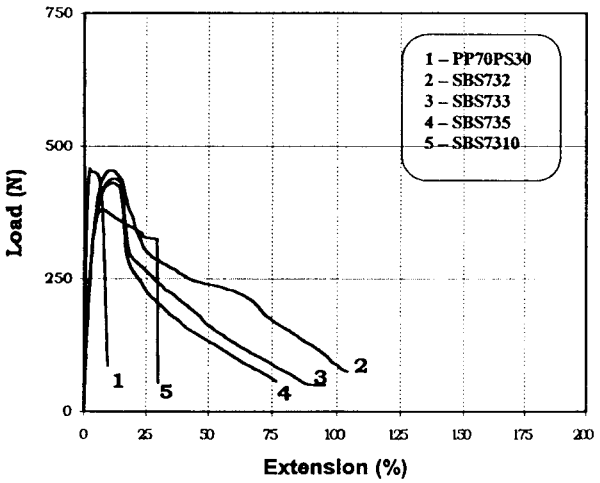

Figure 2 Load–extension curves of the SBS-compatibilized 70/30 PP/PS blends.

with the same rheometer. G' measures the elastic response of a polymer, whereas the loss modulus (G'') measures the energy that dissipates during flow deformation. A frequency sweep test was performed on samples at 190°C over a frequency range of 0.1–40 Hz.

Morphological characterization

The morphologies of the blends were examined with a Philips model XL 30 scanning electron microscope (The Netherlands) with cryogenically fractured specimens in the plane perpendicular to the flow direction of the injection molding. The cryogenically fractured surfaces of the specimens were coated with a thin film of gold for the prevention of charging.

RESULTS AND DISCUSSION

Mechanical properties

Table II contains a summary of the mechanical properties for all the compatibilized blend compositions tested.

Figures 1–3 show the load–extension curves of the SIS-, SBS- and SBR-compatibilized PP/PS blend systems. For the SIS-compatibilized blends, the ductile fracture could be observed at all concentrations of SIS, with the toughness increasing with an increasing amount of SIS. The SBS-compatibilized blends also showed the ductile fracture at all concentrations of SBS, but the toughness decreased with an increasing amount of SBS. In contrast, SBR-compatibilized blends showed brittle fracture at all concentrations of SBR. As can be seen in Table II, the yield stress was reduced marginally and the tensile modulus decreased proportionally with increasing amounts of SIS, SBS, and SBR. This may be due to the electrometric nature of SIS, SBS, and SBR. The yield stress of the SBS-compatibilized blends was higher than that of the SIS- and SBR-compatibilized blends at all concentrations. This indicates that SBS was more effective in compatibilizing the PP/PS blends because it improved the affinity between the phases and dispersion state of the particles. The tensile modulus of the SBR-compatibilized blends was slightly higher than that of SIS- and SBS-compatibilized blends at 3, 5, and 10 phr. The ductility increased substantially with an increasing amount of SIS but decreased considerably with an increasing amount of SBS and SBR. The ductility was much higher for the SIS-compatibilized blends in comparison with the SBS- and SBR-compatibilized blends at all concentrations of the compatibilizers. This may suggest that the effectiveness of SIS as a compatibilizer was less than that of SBS and SBR. As can be seen in Table II, the impact strength increased significantly with an increasing concentration of the compatibilizer for SIS- and SBR-compatibilized blends, whereas the

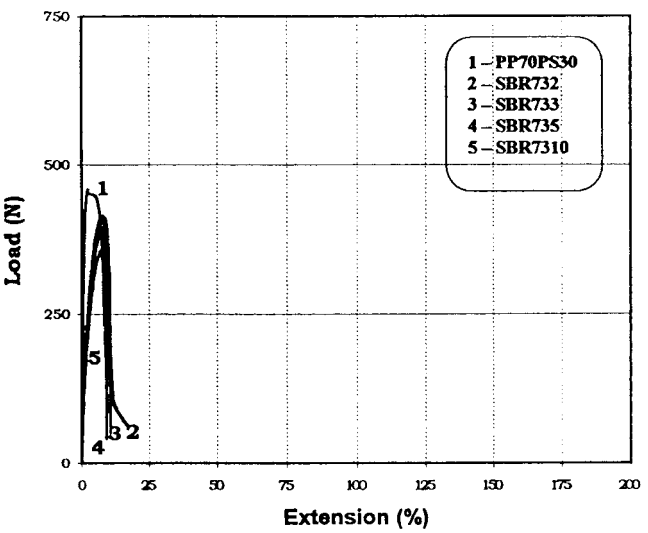

Figure 3 Load–extension curves of the SBR-compatibilized 70/30 PP/PS blends.

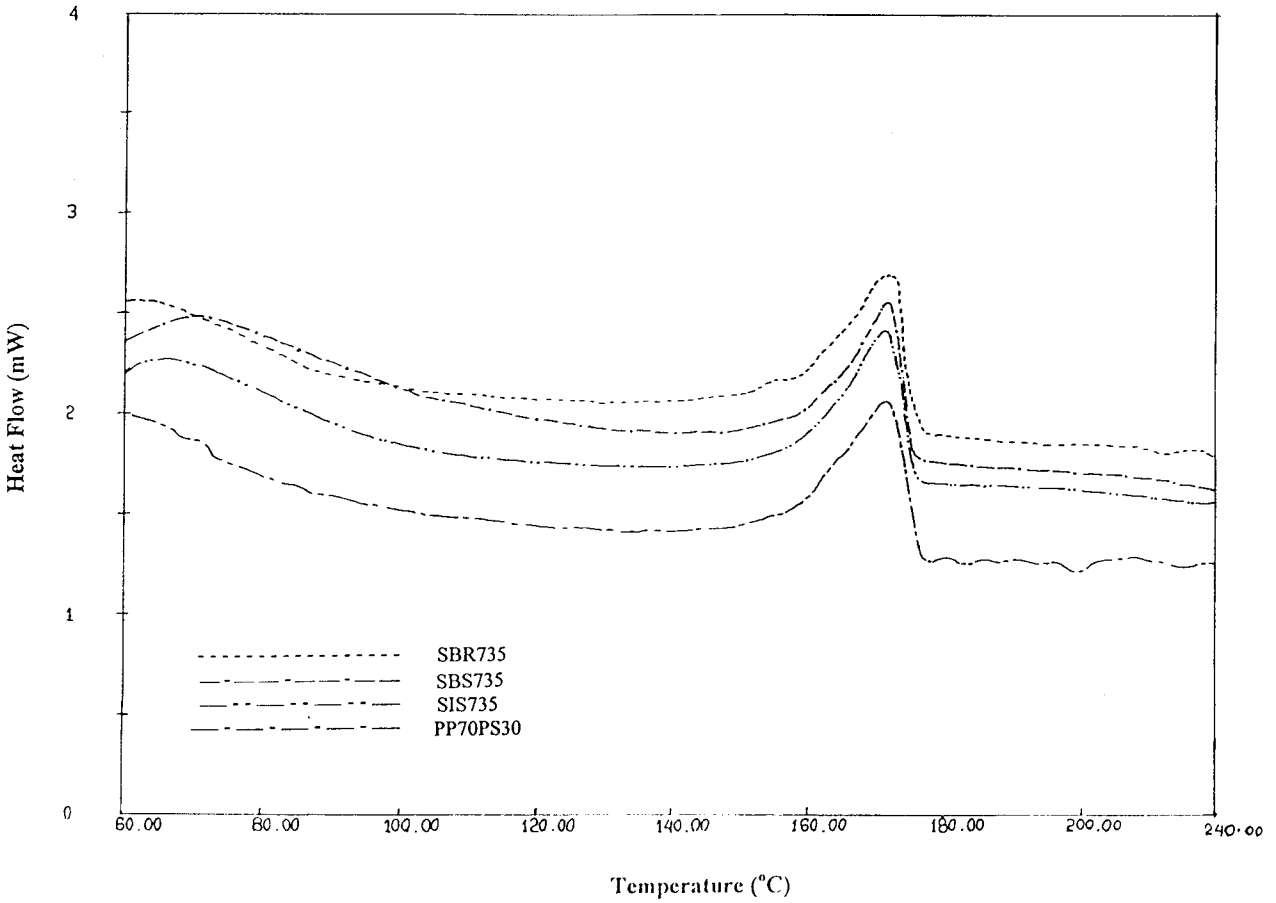

Figure 4 DSC thermograms of 5 phr SIS-, SBS-, and SBR-compatibilized 70/30 PP/PS blends.

increase in the impact strength was marginal for the SBR-compatibilized blends. At 10 phr SBS, the impact strength value reached 2.5 times that of the noncompatibilized blends at the cost of only a 6.2% reduction in the yield stress.

It is clear from Table II that the flexural properties of the SIS-, SBS-, and SBR-compatibilized blends followed the same trend as that of the tensile properties, except at a level of 10 phr compatibilizer, at which concentration the flexural properties were reduced significantly.

The data in Table II clearly indicate that the effects of different amounts of SIS, SBS, and SBR on the linear shrinkage of 70/30 PP/PS blends were negligible.

Thermal analysis

Figure 4 shows differential scanning calorimetry (DSC) thermograms of 5 phr SIS-, SBS-, and SBR-compatibilized 70/30 PP/PS blends. Table III summarizes the DSC results for the PP/PS blends. Because PP was semicrystalline and PS was amorphous in nature, with the addition of PS to PP, the crystallinity percentage of the noncompatibilized blend was decreased on account of the decrease in the enthalpy of melting (ΔH_m) of the PP phase, and the crystalline peak area decreased with an increasing PS content, as can be seen in Figure 4. Similarly, for compatibilized blends,

TABLE III
Summary of the DSC Results for PP/PS Blend Compositions with and Without Compatibilizer

	PP Phase					
Blend code	Onset temperature of melting (°C)	Temperature of melting (°C)	Onset temperature of crystallization (°C)	Temperature of crystallization (°C)	ΔH_m (J/g)	ΔH_c (J/g)
VPP	161.44	172.77	128.56	122.33	85.42	111.20
PPS73	156.70	171.26	125.20	120.65	52.59	68.45
SIS735	159.07	170.64	123.20	119.00	46.73	58.52
SBS735	160.36	171.35	122.86	117.60	45.66	56.27
SBR735	160.39	172.36	123.23	119.43	45.25	57.74

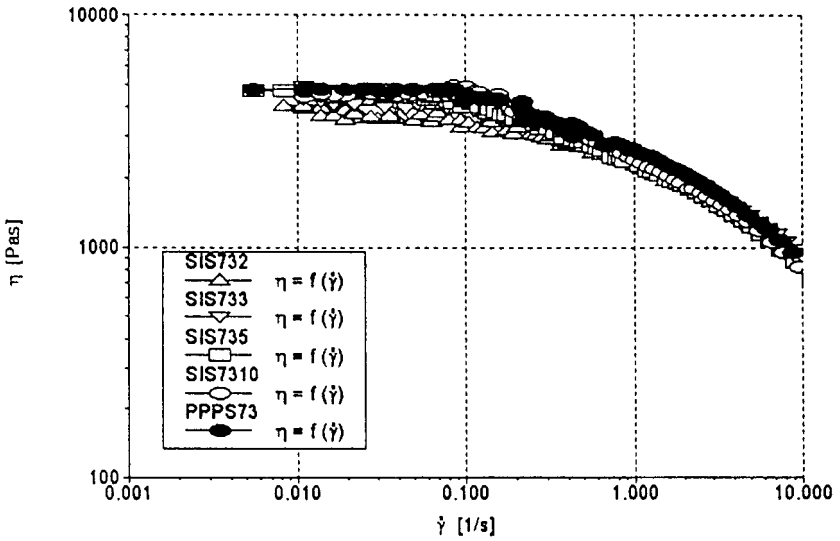

Figure 5 Flow curves of the SIS-compatibilized 70/30 PP/PS blends at 200°C.

with the incorporation of SIS, SBS, and SBR, there was a further reduction in ΔH_m and in the enthalpy of crystallization (ΔH_c); this confirmed that there was some sort of compatibilization between PP and PS and, therefore, a further reduction in the degree of crystallization of PP. The addition of 5 phr SBS and SBR to the 70/30 PP/PS blend shifted the melting temperature of PP toward the melting range of PS. The addition of 5 phr SIS to the blend showed the opposite trend, and this indicated that its compatibilizing action was poor in comparison with that of SBS and SBR. The same observation was also supported by a decrease in the impact strength

E

The results for E are presented in Table II. The MFI is an indirect measure of viscosity. Therefore, MFI values at different temperatures can be used to calculate E at a particular load that corresponds to a particular shear rate. E is one of the most important molecular parameters. It gives valuable insight into the structures of polymers. It provides an analytical method[23] for differentiating different polymer types and structural changes within a given polymer type.

The temperature dependency of the MFI can be stated with the following Arrhenius equation:

$$\text{MFI} = Ae^{-E/RT}$$

where A is a constant and R and T are the universal gas constant and absolute temperature, respectively. E, which can be calculated from the slope obtained by the linear regression of log MFI versus $1/T$, is shown in Table II for PP/PS blend systems.

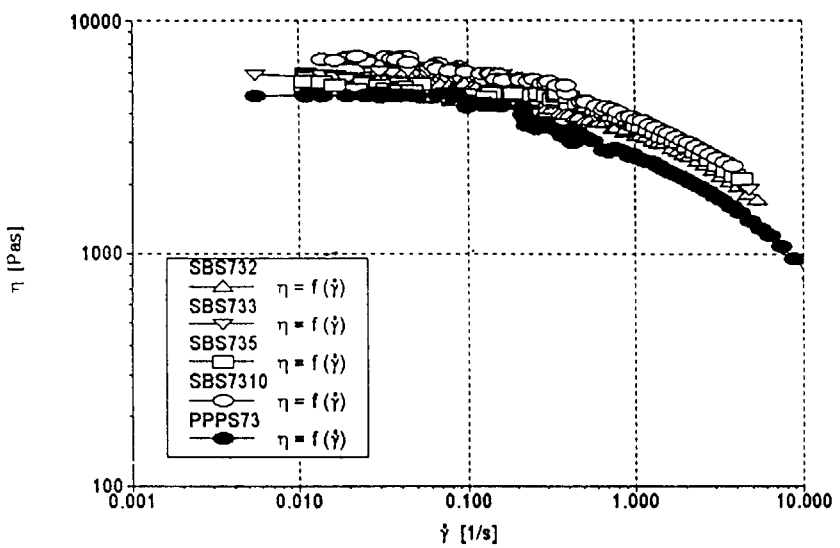

Figure 6 Flow curves of the SBS-compatibilized 70/30 PP/PS blends at 200°C.

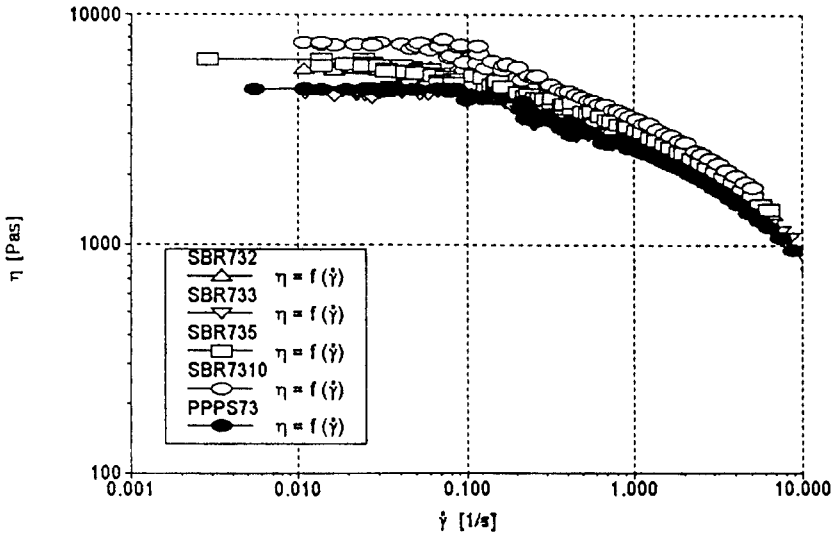

Figure 7 Flow curves of the SBR-compatibilized 70/30 PP/PS blends at 200°C.

The data from Table II clearly show that SIS-, SBS-, and SBR-compatibilized 70/30 PP/PS blends had higher E values than the noncompatibilized blend. This was due to the increased interaction between the two phases upon the addition of the compatibilizers, which enhanced E. The data also indicate that E of the SBS-compatibilized blend was higher at all concentrations of the compatibilizer in comparison with the values for SIS- and SBR-compatibilized blends. This clearly explains the increased compatibilizing effect of SBS in the PP/PS blends. E of virgin PP was reduced upon the addition of SBR, and this reduction in E was marginal until an SBR content of 5 phr; thereafter, it fell significantly. This may be due to the dispersion of SBR in the blend, which induced the disentanglement or deformation of entanglement networks of the continuous PP phase, which led to a reduction of E. E of the SBR-compatibilized 90/10 PP/PS blend followed the same trend as that of the 70/30 PP/PS blends.

Viscous behavior

From the point of view of polymer processing, theoretical predictions of the rheological properties of

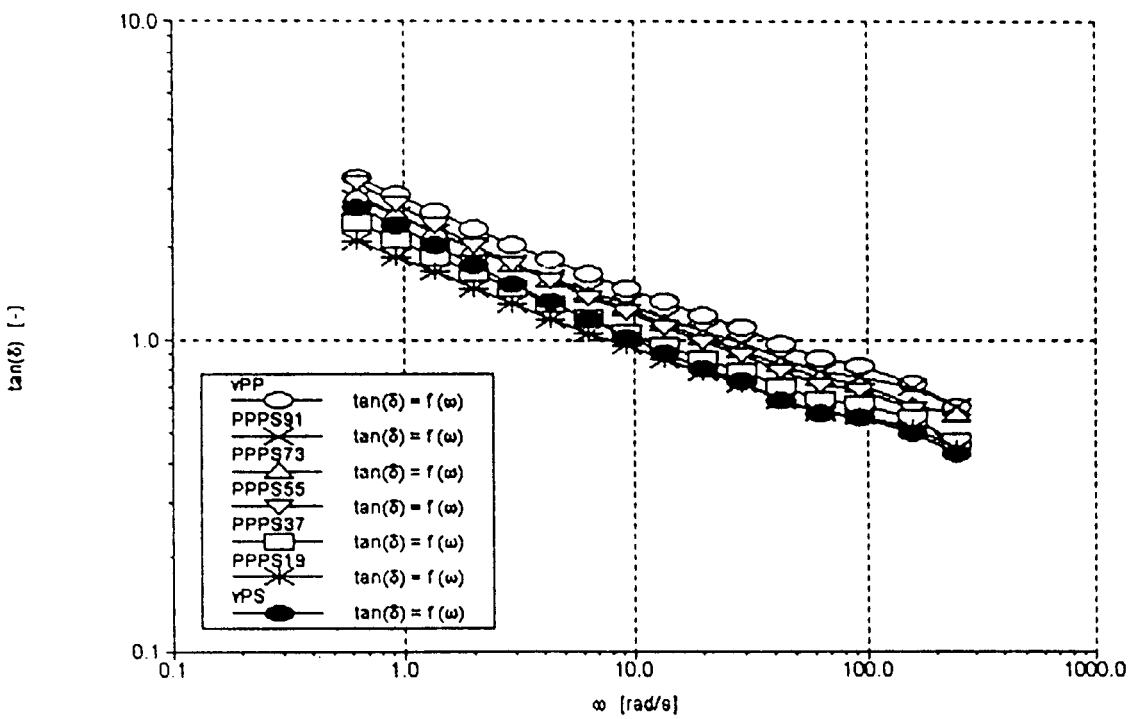

Figure 8 Variations of tan δ with frequency (ω) for noncompatibilized PP/PS blends at 190°C.

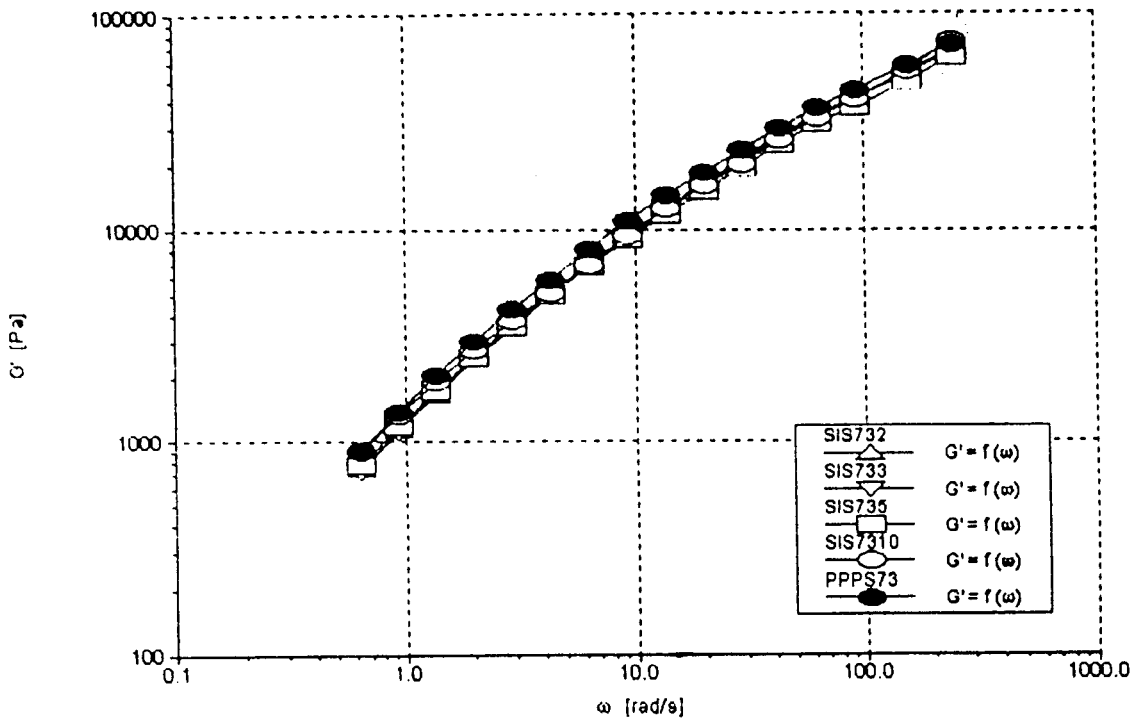

Figure 9 Variations of G' with frequency (ω) for SIS-compatibilized 70/30 PP/PS blends at 190°C.

polymers and their blends are essential. Figures 5–7 show the variations of the shear viscosity (η) with the shear rates ($\dot{\gamma}$) for 70/30 PP/PS blends compatibilized with different amounts of SIS, SBS, and SBR. The figures show that the flow curves of the SIS-compatibilized blends lay below that of the noncompatibilized blend at all concentrations of the compatibilizer; this indicates the reduction in viscosity upon the addition of SIS. This may be due to the insufficient compatibilizing effect of SIS. The flow curves of SBS- and SBR-compatibilized blends lay above that of the noncompatibilized blend at all concentrations of the compatibilizers. This clearly demonstrates that SBS and SBR provided good compatibility in the PP/PS blends. The

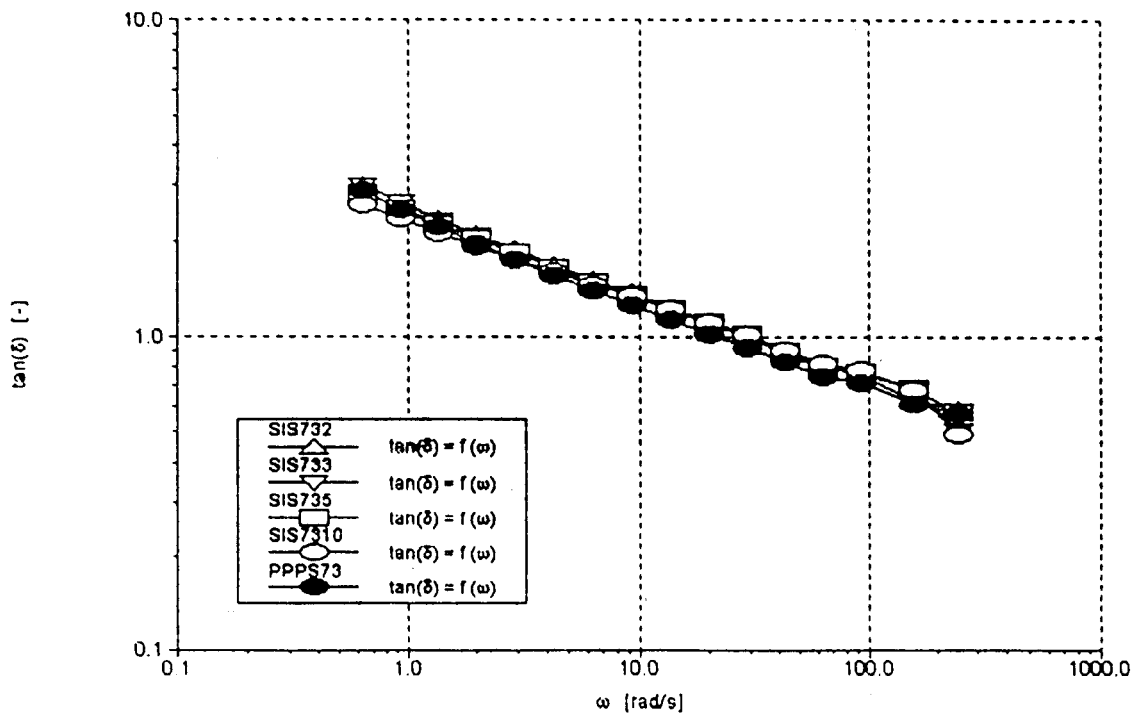

Figure 10 Variations of tan δ with frequency (ω) for SIS-compatibilized 70/30 PP/PS blends at 190°C.

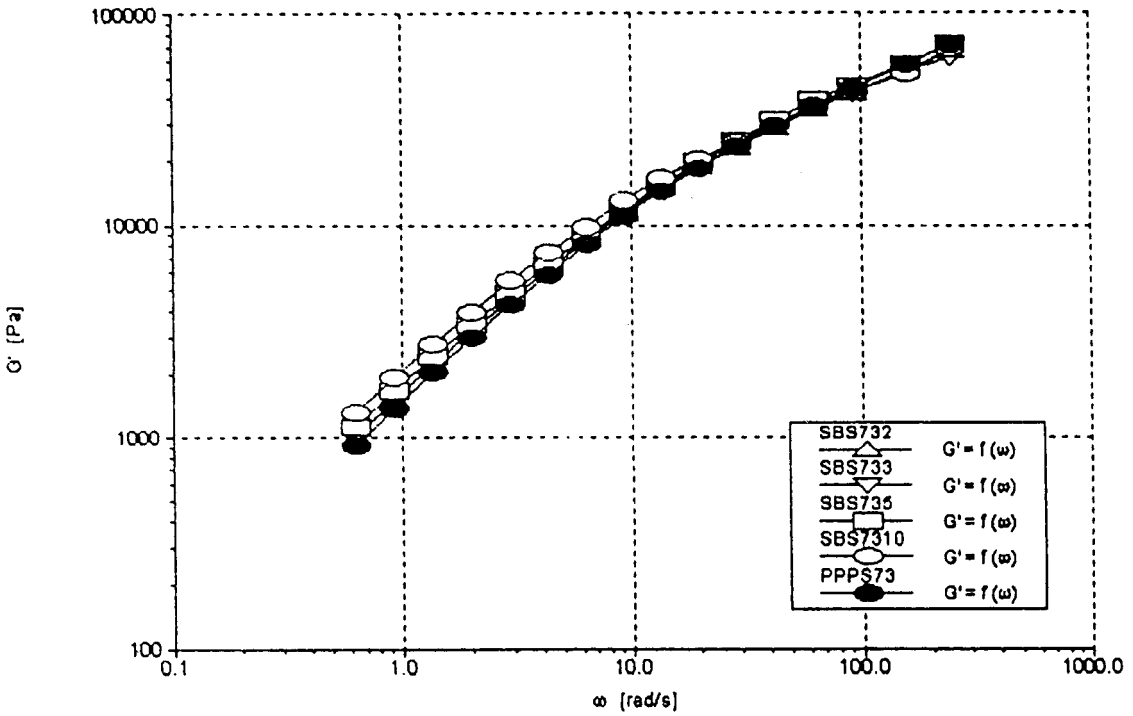

Figure 11 Variations of G' with frequency (ω) for SBS-compatibilized 70/30 PP/PS blends at 190°C.

viscosity of the 70/30 blends with 10 phr SBS and SBR appeared to be highest, whereas the same blend with 10 phr SIS appeared to have the lowest viscosity. SBS- and SBR-compatibilized blends showed higher melt viscosity than SIS-compatibilized blends. Therefore, the results indicate that SBS and SBR provided compatibility at all concentrations.

Dynamic shear test analysis

Figures 8–14 show the dynamic viscous behavior of SIS-, SBS-, and SBR-compatibilized PP/PS blends. As can be seen in Figures 8, 10, and 12, the addition of SIS to 70/30 PP/PS blends did not affect the G' values up to a level of 10 phr over the entire frequency range. However,

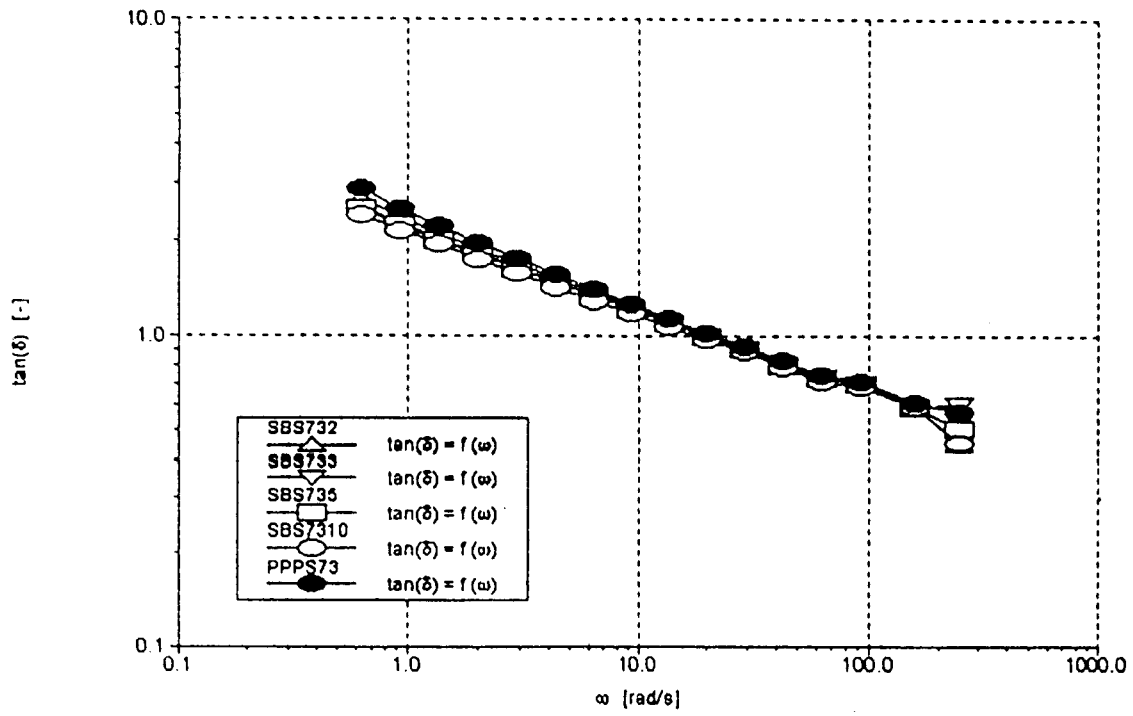

Figure 12 Variations of tan δ with frequency (ω) for SBS-compatibilized 70/30 PP/PS blends at 190°C.

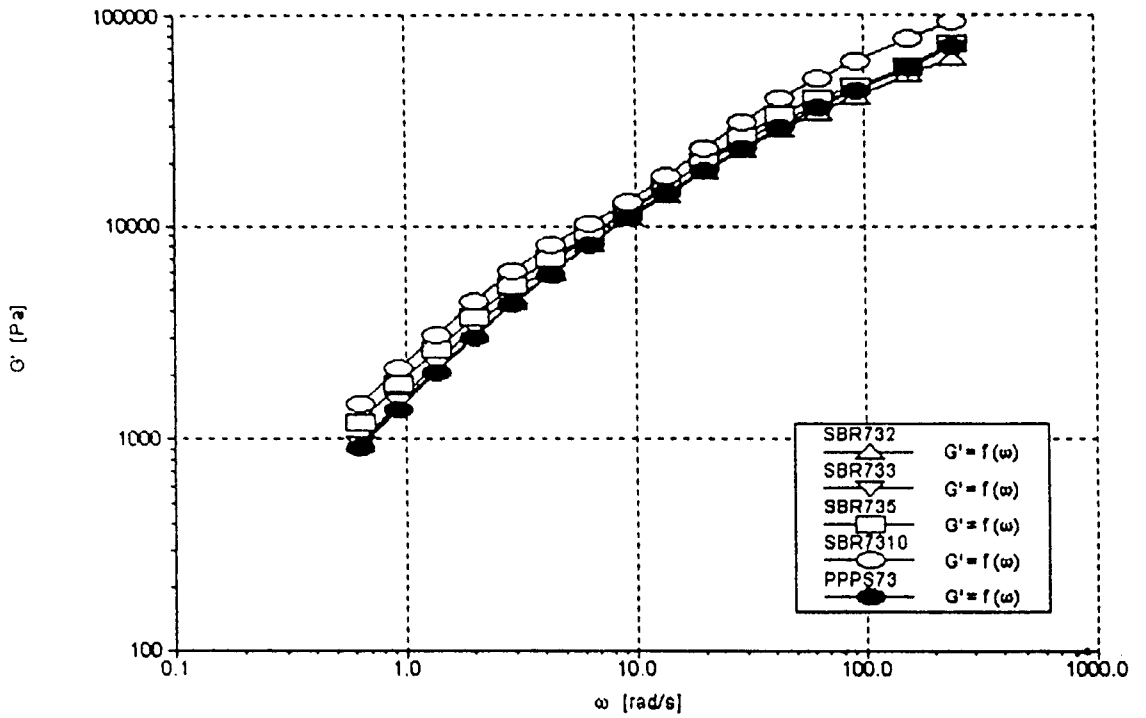

Figure 13 Variations of G' with frequency (ω) for SBR-compatibilized 70/30 PP/PS blends at 190°C.

the addition of SBS showed marginally higher G' values at a low-frequency region, whereas the addition of SBR showed increased G' values depending on the amount of SBR over the entire frequency range.

To further understand the viscoelastic properties of the polymer, we calculated tan δ values. Tan δ is the ratio of G'' to G' of a polymer. If tan δ is greater than unity, the viscous component of the deformation dominates, and the polymer will behave as a viscous fluid. The polymer will behave as an elastic solid when tan δ is less than unity. For thermoforming, a polymer sheet must have a sufficiently elastic component to resist sagging, but it must remain viscous enough to flow into the mold under stress.[24] Therefore, a good

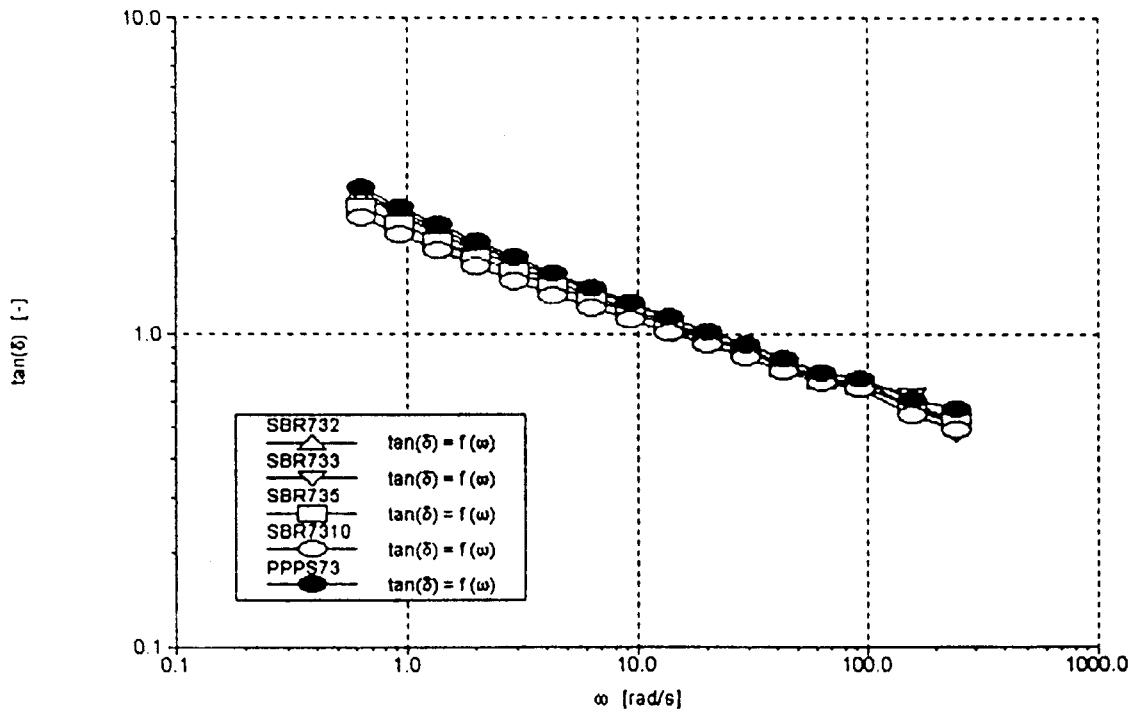

Figure 14 Variations of tan δ with frequency (ω) for SBR-compatibilized 70/30 PP/PS blends at 190°C.

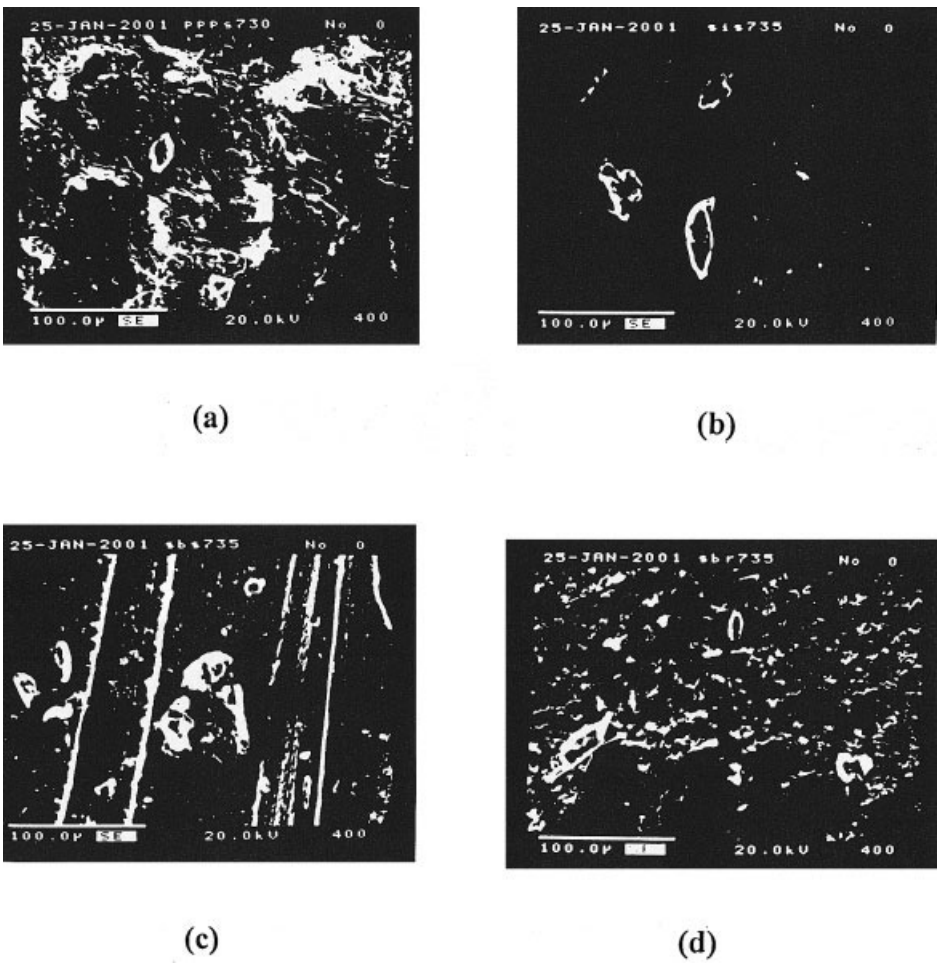

Figure 15 SEM images of (a) a 70/30 PP/PS blend without a compatibilizer, (b) a 70/30 PP/PS blend with 5 phr SIS, (c) a 70/30 PP/PS blend with 5 phr SBS, and (d) a 70/30 PP/PS blend with 5 phr SBR.

thermoforming material must have both viscous and elastic components at the forming temperature. Figures 9, 11, and 13 demonstrate that the addition of SIS, SBS, and SBR did not influence the tan δ values at a high-frequency region. The SBR-compatibilized blends showed a tan δ value closer to unity than the SIS- and SBS-compatibilized blends at a frequency of 10 rad/s; this indicated the suitability of SBR-compatibilized 70/30 PP/PS blends for thermoforming.

Morphology

Figure 15 shows the morphology of noncompatibilized and 5 phr compatibilized SIS-, SBS-, and SBR-compatibilized 70/30 PP/PS blends at a 400× magnification. For the noncompatibilized 70/30 blends, the morphology seemed to be distinguished by a large domain size of the dispersed phase with relatively large particles protruding from the matrix. The scanning electron microscopy (SEM) image also shows the complete nonwetting of PP and PS. This is evidence that the interfacial interaction between the two phases was very weak because of the structural difference between the dispersed phase (PS polar) and the continuous phase (PP nonpolar). In contrast, Figure 15(b–d) shows blends containing 5 phr SIS, SBS, and SBR in which the particles were embedded within the matrix; this also seemed to reduce the domain size considerably. Therefore, the addition of a compatibilizer increased the dispersion and particle size distribution of PS in PP by reducing the size of the particle. SBS and SBR provided better dispersion and better wetting of PS than SIS, leading to improved adhesion to the PP matrix. This may suggest that the SIS-compatibilized blends had limited compatibility.

CONCLUSIONS

The following conclusions can be drawn from this investigation of PP/PS blends compatibilized with SIS, SBS, and SBR. The use of SBS enhanced the toughness, ductility, and impact strength, whereas the use of SIS increased the elongational properties, toughness, and impact strength while reducing the yield stress. The melt viscosity and G' values of the PP/PS blends depended on the type and amount of compatibilizer. All the compatibilized PP/PS blend compositions showed well-defined zero shear viscosity and

pseudoplastic behavior. The SBR-compatibilized blends showed tan δ values closer to unity than the SBS- and SIS-compatibilized blends, and this indicated the suitability of these blends for thermoforming. The high tan δ values of the SIS- and SBS-compatibilized blends showed that these polymers had a greater tendency to sag during thermoforming.

The DSC study confirmed that the addition of SIS, SBS, and SBR shifted the melt peak of PP toward the melting range of PS, thereby indicating the compatibilizing effect.

SEM images showed a large domain size of the dispersed phase for the noncompatibilized 70/30 PP/PS blends and a significantly decreased domain size for the SIS-, SBS-, and SBR-compatibilized PP/PS blends.

The authors acknowledge Reliance Industries and Supreme Petrochem for providing the raw material.

References

1. Jagtap, R. N.; Nere, C. K. Popular Plast Packaging 2001, 46, 68.
2. Jaishankar, S. S.; Radhakrishnan, G. Polym Eng Sci 2000, 40, 621.
3. Paul, D. R.; Barlow, J. W. Polymer 1984, 25, 487.
4. Xanthos, M. Polym Eng Sci 1988, 28, 1392.
5. Gaylord, N. G. J Macromol Sci Chem 1989, 26, 1211.
6. Durst, R. R. U.S. Pat. 3,907,929 (1975).
7. Kawai, H.; Munemaru, T.; Inoue, T.; Kimura, R. Jpn. Pat. JP 043,539 (1978).
8. Holden, G.; Gouw, L. H. Eur. Pat. Appl. EP 004,685 (1979).
9. Siegfried, D. L.; Thomas, D. A.; Sperling, L. H. U.S. Pat. 4,468,499 (1984).
10. Grancio, M. R.; Steward, O. F.; Cass, J. F. U.S. Pat. 4,386,187 (1985).
11. Xu, G.; Lin, S. Polymer 1996, 37, 421.
12. Ha, C. S.; Park, H. D.; Kim, Y.; Kwon, S. K.; Cho, W. J. P. Polym Adv Technol 1997, 7, 483.
13. Santana, O. O.; Muller, A. J. Polym Bull 1994, 32, 471.
14. Mitsuyoshi, F. J Appl Polym Sci 1997, 63, 1015.
15. Smit, I.; Radonjic, G. Polym Eng Sci 2000, 40, 2144.
16. Iwala, I.; Yoshimura, M.; Ishifda, Y.; Tanaka, K.; Deki, T. Proceedings of Mitsui-Toatsu, Chemical and Mechanical Behavior of Materials—VI, Kyoto, Japan, July 29–Aug 2, 1991; p 295.
17. Pluta, M.; Morawiec, J.; Kryszewski, M.; Kowalewski, I. J Therm Anal 1996, 46, 1061.
18. Rablej, S. Eur Polym J 1993, 129, 625.
19. Fortelny, I.; Michalkova, D.; Mikesova, J. J Appl Polym Sci 1996, 59, 155.
20. Del Giudice, L.; Cohen, R. E.; Attalla, G.; Bertinotti, F. J Appl Polym Sci 1985, 30, 4305.
21. Appleby, T.; Cser, F.; Maod, G.; Rizzardo, E.; Starropoulos, C. Polym Bull 1994, 32, 479.
22. D'Orazio, L.; Guarino, R.; Mancarella, C.; Martuscelli, E.; Cecchin, G. J Appl Polym Sci 1999, 72, 1429.
23. Rohn, C. L. Analytical Polymer Rheology, 1st ed.; Munich-Hanser: Munich, 1995; p 142.
24. Macauley, N.; Harkin-Jones, E.; Murphy, W. R. Plast Eng 1996, 52(7), 33.